High-Speed Shielding Current Analysis in High-Temperature Superconducting Film with Cracks

Atsushi Kamitani[1], Teruou Takayama[2], and Ayumu Saitoh[3]

[1]Graduate School of Science and Engineering, Yamagata University, Yonezawa, Yamagata 992-8510 JAPAN
[2]Faculty of Engineering, Yamagata University, Yonezawa, Yamagata 992-8510 JAPAN
[3]Graduate School of Engineering, University of Hyogo, Himeji, Hyogo 671-2280, JAPAN

A fast and stable method is proposed for calculating the shielding current density in a high-temperature superconducting film containing cracks. After discretized with the finite element method, the initial-boundary-value problem of the shielding current density reduces to semi-explicit differential algebraic equations (DAEs). Although the DAEs can be solved with standard ordinary-differential-equation (ODE) solvers, much CPU time is required for its numerical solution. In order to shorten the CPU time, a high-speed method is proposed. In the method, the block LU decomposition is incorporated into function evaluations in ODE solvers. A numerical code is developed on the basis of the proposed method and, as an application of the code, detectability of cracks by the scanning permanent-magnet method is numerically investigated.

***Index Terms*—Critical current density, differential algebraic equations, high-temperature superconductors, surface crack**

I. Introduction

RECENTLY, a high-temperature superconductor (HTS) has been used for numerous engineering applications: magnet, energy storage system, power cable and magnetic shielding apparatus. Since evaluation of the shielding current density is indispensable for the design of engineering applications, several numerical methods [1]–[3] have been so far proposed to calculate the shielding current density.

After discretized with the implicit scheme and the finite element method (FEM), an initial-boundary-value problem of the shielding current density is transformed to a problem in which nonlinear algebraic equations have to be solved at each time step. Although this method can be also applied to the shielding current analysis in an HTS film containing cracks, it is extremely time-consuming. This method is called a virtual voltage method [2], [4].

The purpose of the present study is to develop a fast and stable method for analyzing the shielding current density in an HTS film containing cracks and to numerically investigate the scanning permanent-magnet method (SPM) [4], [5].

II. Governing Equations

We first assume that an HTS film has the same cross section Ω over the thickness and that it is exposed to the time-varying magnetic field $\boldsymbol{B}/\mu_0$. Furthermore, the HTS film is assumed to contain m cracks whose cross sections are curved segments in the xy plane. Note that the boundary $\partial\Omega$ of Ω is composed of not only the outer boundary C_0 but also crack surfaces $C_1, C_2, \cdots, C_m$. In the following, $\boldsymbol{x}$ and $\boldsymbol{x}'$ denote position vectors of two points in the xy plane and $\boldsymbol{t}$ is a unit tangent vector on $\partial\Omega$. In addition, b denotes a film thickness.

In HTS films, the electric field $\boldsymbol{E}$ and the shielding current density $\boldsymbol{j}$ are closely related to each other through the J-E constitutive relation. As the relation, we assume the following power law [2]–[4], [6]: $\boldsymbol{E} = E_{\mathrm{C}}(|\boldsymbol{j}|/j_{\mathrm{C}})^N [\boldsymbol{j}/|\boldsymbol{j}|]$, where j_{C} and E_{C} denote the critical current density and the critical electric field, respectively, and N is a positive constant.

Under the thin-plate approximation, there exists a scalar function $T(\boldsymbol{x}, t)$ such that $\boldsymbol{j} = (2/b)\nabla \times (T\boldsymbol{e}_z)$, and its time evolution is governed by the following equation [1], [2], [4]:

$$\mu_0 \frac{\partial}{\partial t}(\hat{W}T) = -(\nabla \times \boldsymbol{E}) \cdot \boldsymbol{e}_z - \frac{\partial}{\partial t}\langle \boldsymbol{B} \cdot \boldsymbol{e}_z \rangle. \tag{1}$$

Here, $\langle\ \rangle$ denotes an average operator over the thickness and the definition of $\hat{W}$ is given in [4].

The initial and boundary conditions to (1) are assumed as follows: $T = 0$ at $t = 0$, $T \in H(\bar{\Omega})$, and $h_i(\boldsymbol{E}) \equiv \oint_{C_i} \boldsymbol{E} \cdot \boldsymbol{t}\, ds = 0$ $(i = 1, 2, \cdots, m)$. Here, $H(\bar{\Omega})$ is a function space defined by $H(\bar{\Omega}) \equiv \{w(\boldsymbol{x}) : w = 0 \text{ on } C_0,\ \partial w/\partial s = 0 \text{ on } \cup_{i=1}^{m} C_i\}$, and s is an arclength along crack surfaces $C_1, C_2, \cdots, C_m$.

III. Numerical Methods

After spatially discretized with the FEM, the initial-boundary-value problem of (1) reduces to the following semi-explicit differential algebraic equations:

$$\begin{bmatrix} W_{11} & W_{12} \end{bmatrix} \frac{d\boldsymbol{T}}{dt} = \boldsymbol{f}_1(t, \boldsymbol{T}), \quad \boldsymbol{g}(\boldsymbol{T}) = \boldsymbol{0}, \tag{2}$$

where $\boldsymbol{T} \in \mathbb{R}^n$ is a nodal vector originating from $T(\boldsymbol{x}, t)$ and $\boldsymbol{f}_1(t, \boldsymbol{T}) \in \mathbb{R}^{n-m}$ is a vector calculated from the right-hand side of (1). Here, n denotes a total number of nodes and it is assumed to satisfy $n \gg m$. In addition, W_{11} and W_{12} are an $(n-m) \times (n-m)$ matrix and an $(n-m) \times m$ matrix, respectively, and $\boldsymbol{g}(\boldsymbol{T}) \in \mathbb{R}^m$ is a vector corresponding to $h_i(\boldsymbol{E}) = 0$ $(i = 1, 2, \cdots, m)$. Incidentally, (1) is obtained by means of an integral approach and, hence, discretization of an air region is unnecessary.

Since (2) shows an index-1 property, it can be rewritten as the following ordinary differential equations:

$$\frac{d\boldsymbol{T}}{dt} = \boldsymbol{f}(t, \boldsymbol{T}), \tag{3}$$

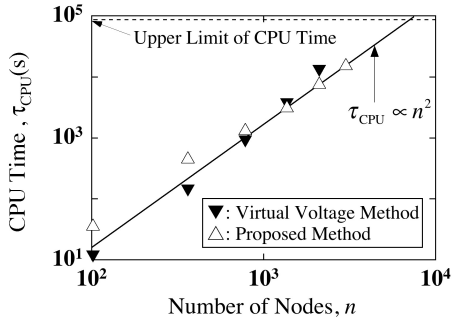

Fig. 1. The CPU time τ_{CPU} as functions of the number n of nodes for the case with $m = 1$. Here, τ_{CPU} is measured for the simulation of the SPM in which values of parameters in Section IV are used.

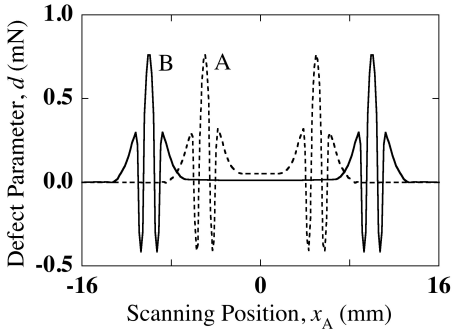

Fig. 2. Dependences of the defect parameter d on the scanning position x_{A}. Here, A: $a = 10$ mm and B: $a = 20$ mm.

where $\boldsymbol{f}(t, \boldsymbol{T}) \in \mathbb{R}^n$ is defined by

$$W(\boldsymbol{T})\boldsymbol{f}(t, \boldsymbol{T}) = \boldsymbol{f}^*(t, \boldsymbol{T}). \tag{4}$$

Here, $W(\boldsymbol{T})$ and $\boldsymbol{f}^*(t, \boldsymbol{T})$ are given by

$$W(\boldsymbol{T}) = \begin{bmatrix} W_{11} & W_{12} \\ W_{21}(\boldsymbol{T}) & W_{22}(\boldsymbol{T}) \end{bmatrix}, \quad \boldsymbol{f}^*(t, \boldsymbol{T}) = \begin{bmatrix} \boldsymbol{f}_1(t, \boldsymbol{T}) \\ \boldsymbol{0} \end{bmatrix}.$$

In addition, $W_{21}(\boldsymbol{T})$ and $W_{22}(\boldsymbol{T})$ are an $m \times (n - m)$ matrix and an $m \times m$ matrix, respectively, and they are given by $\begin{bmatrix} W_{12}(\boldsymbol{T}) & W_{22}(\boldsymbol{T}) \end{bmatrix} = \partial \boldsymbol{g}/\partial \boldsymbol{T}$, where $\partial \boldsymbol{g}/\partial \boldsymbol{T}$ is a Jacobian matrix. In the present study, the initial-value problem of (3) is numerically solved by means of the 5th-order Runge-Kutta method with the adaptive step-size control algorithm [7].

In the 5th-order Runge-Kutta method, 6 evaluations of $\boldsymbol{f}(t, \boldsymbol{T})$ are needed at each time step. In other words, 6 linear systems such as (4) have to be solved for $\boldsymbol{f}(t, \boldsymbol{T})$ at each time step. As is apparent from the definition of $W(\boldsymbol{T})$, neither W_{11} nor W_{12} depends on $\boldsymbol{T}$. Hence, if we have already obtained the LU decomposition of W_{11}, $O(n^2)$ operations are required for solving (4). This means that only $O(n^2)$ operations are needed at each time step of the proposed method. In contrast, $O(n^3)$ operations are necessary at each time step of the virtual voltage method.

Let us compare the speed of the proposed method with that of the virtual voltage method. The dependence of the CPU time τ_{CPU} on the number of nodes is depicted in Fig. 1. As expected, the proposed method is faster than the virtual voltage method for the case with $n \gtrsim 10^3$. Especially, for the case with $n = 3007$, the execution of the virtual voltage method was forced to be terminated because the CPU time had exceeded the upper limit, 8.64×10^4 s. Hence, for this case, the proposed method is over 5.3 times faster than the virtual voltage method. From these results, we can conclude that the proposed method could be effective especially for a large-sized shielding current analysis in an HTS film containing cracks.

IV. Application to SPM

On the basis of the method explained above, a high-speed numerical code has been developed for analyzing the time evolution of $\boldsymbol{j}$. By using the code, crack detection with the SPM is investigated. In the following, Ω is assumed to be a rectangle of length l and width w, and its longitudinal direction is taken as x-axis. In addition, cross sections of two cracks are assumed to be the following two line segments in the xy plane: a line segment connecting two points, $(-a/2, \pm L_{\mathrm{c}}/2)$, and a line segment connecting two points, $(a/2, \pm L_{\mathrm{c}}/2)$.

In the SPM, a cylindrical permanent magnet of radius R and height H is moved along the film surface and, simultaneously, an electromagnetic force acting on the film is monitored. In the following, the symmetry axis of the magnet is denoted by $(x, y) = (x_{\mathrm{A}}, y_{\mathrm{A}})$, and its movement is assumed as $x_{\mathrm{A}} = \pm(vt - l/2) \equiv x_{\pm}(t)$ and $y_{\mathrm{A}} = \text{const}$. Here, v is a scanning speed. The physical and geometrical parameters are fixed as follows: $R = 0.8$ mm, $H = 2$ mm, $j_{\mathrm{C}} = 1.0$ MA/cm^2, $E_{\mathrm{C}} = 1$ mV/m, $N = 20$, $b = 1$ μm, $l = 32$ mm, $w = 10$ mm, $L_{\mathrm{c}} = 2$ mm, $y_{\mathrm{A}} = 0$ mm, and $v = 10$ cm/s.

Let us numerically investigate whether or not two cracks can be distinguished by the SPM. Dependences of the defect parameter d [4] on x_{A} are numerically determined for $a = 10$ mm and for $a = 20$ mm, and they are depicted in Fig. 2. This figure indicates that $|d|$ does not vanish even at $x_{\mathrm{A}} = 0$ mm for the case with $a = 10$ mm. In contrast, $|d| \cong 0$ mN is fulfilled there for the case with $a = 20$ mm. In other words, two cracks are regarded as a single crack for the case with $a = 10$ mm, whereas they are completely distinguishable for the case with $a = 20$ mm. This result implies that multiple cracks will remarkably affect resolution of the SPM.

References

[1] Y. Yoshida, M. Uesaka, and K. Miya, "Magnetic-field and force analysis of high-T_{c} superconductor with flux-flow and creep," *IEEE. Trans. Magn.*, vol. 30, no. 5, pp. 3503-3506, Sep. 1994.

[2] A. Kamitani, T. Takayama, and S. Ikuno, "Virtual voltage method for analyzing shielding current density in high-temperature superconducting film with cracks/holes," *IEEE Trans. Magn.*, vol. 49, no. 5, pp. 1877-1880, May 2013.

[3] A. Kameni *et al.*, "A 3-D semi-implicit method for computing the current density in bulk superconductors," *IEEE. Trans. Magn.*, vol. 50, no. 2, Art. No. 7009204, Feb. 2014.

[4] A. Kamitani, T. Takayama, and A. Saitoh, "Numerical investigations on applicability of permanent magnet method to crack detection in HTS film," *Physica C*, vol. 504, pp. 57-61, Sep. 2014.

[5] K. Hattori *et al.*, "Detection of smaller J_{c} region and damage in YBCO coated conductors by using permanent magnet method," *Physica C*, vol. 471, no. 21, pp. 1033-1035, Nov. 2011.

[6] R. Brambilla, F. Grilli, and L. Martini, "Integral equations for computing AC losses of radially and polygonally arranged HTS thin tapes," *IEEE Trans. Appl. Supercond.*, vol. 22, vol. 4, Art. No. 8401006, Aug. 2012.

[7] W. H. Press, S. A. Teukolsky, W. T. Vetterling, and B. P. Flannery, *Numerical Recipes in Fortran 77*, 2nd ed., New York, NY, USA: Cambridge Univ. Press, 1992, pp. 708-716.